The ISO-SWS Relative Spectral Response Calibration

Prepared by: Bart Vandenbussche (SIDT/KUL)
Bart.Vandenbussche@ster.kuleuven.ac.be

1 Introduction

This document describes how the Relative Spectral Response Function (RSRF) calibration of the ISO-SWS was done in the course of the mission.

Before launch, the Relative Spectral Response of the SWS in all AOT bands was derived from blackbody scans during ILT tests. Uncertainties in blackbody temperatures, diffraction losses and leaks in test setup filters made a correction of the Relative Spectral Response function (RSRF) necessary, based on what was observed in-orbit on external calibrators. In the course of the mission different correction methods were developed, in order to correct only for the effects that are understood to be instrumental. This document describes in chronological order the different corrections that were applied in different versions of the pipeline.

We also indicate where further improvements in the RSRF can be expected.

Appendix A gives details about the synthetic spectra referenced in the document. Appendix B describes the so-called CAP : The Calibration Procedure that describe how the calibration file derivations can be implemented with Interactive Analysis (IA) commands and routines.

2 OLP 8.4 (and higher) RSRF calibration and quality

The present version of IA-BASE, OSIA (v1.0 an higher), and the on-the-fly re-processing at the ISO-data center in Vilspa (OLP 8.4 and higher) uses versions 040 of the Cal25 RSRF calibration files. The derivation and quality of these calibration files is described in section 5 (Derivation of ILT RSRFs that were the basis for further corrections), section 6 (How these ILT RSRFs were corrected for instrumental effects seen in SWS observations of stellar standards), section 7 (An overview of the RSRF for all bands, together with an indication of the reliability in different wavelength regions), and section 8, where we show how shapes in the RSRF can propagate to the final spectrum after a slightly wrong dark current subtraction, and how the observer can recognize and cure such a problem.

3 Correction for a leak in the ILT setup filters

A first correction was introduced in May 1996 in the RSRF for bands 1a and 2a. A sudden fall-off was seen at the blue side of these bands in all observations. An Alfa Lyrae observation was taken as a representative case. A RSRF for 1a and 2a was derived from Alfa Lyrae by dividing the dark subtracted SPD by a Cohen template (HR7001_M_COHEN). A polynomial fit of the difference between ILT RSRF and the Alfa Lyrae RSRF was then the correction that was applied.

Figure 1 and Figure 2 show the difference between the RSRF before and after the correction in bands 1a and 2a resp.

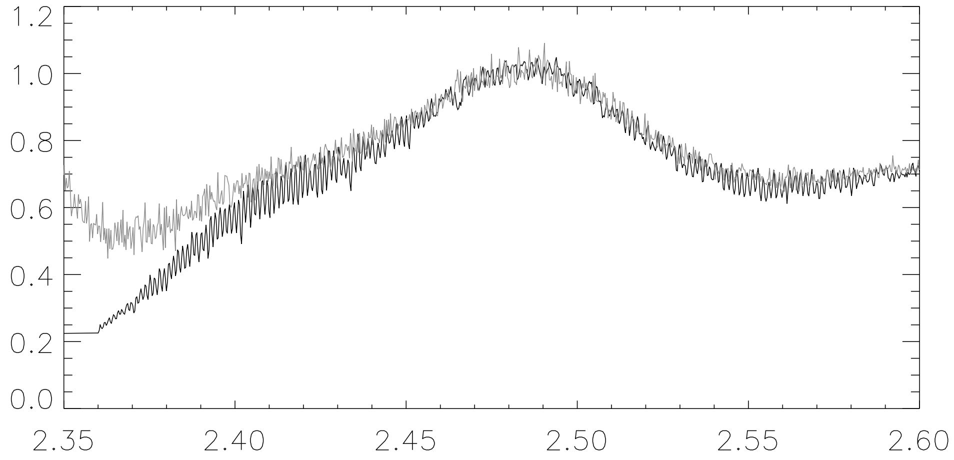

Figure 1: The difference between the RSRF before and after the first in-orbit correction for band 1a.

The resulting calibration files are available in IA as CAL25_1A_010 and CAL25_2A_010.

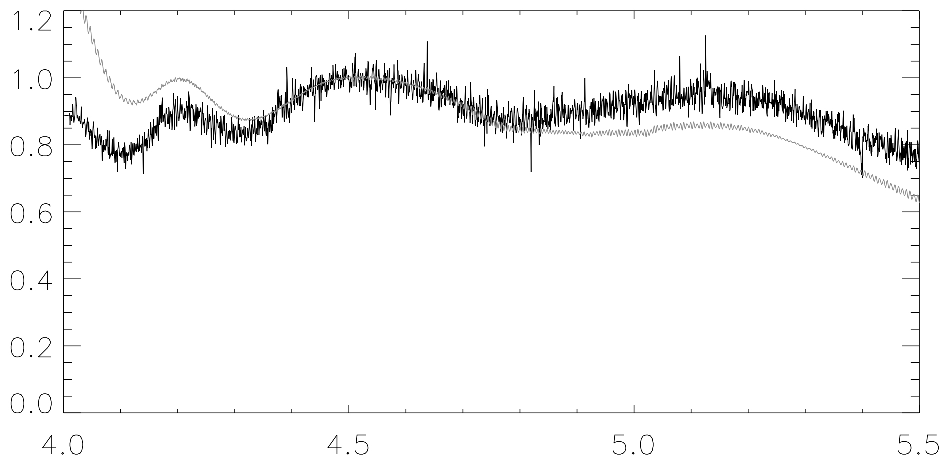

Figure 2: The difference between the RSRF before and after the first in-orbit correction for band 2a.

4 Polynomial Broadband corrections

The RSRF was intensively measured in the lab during the pre-launch tests at Instrument Level. The calibration source used was a cryogenic black-body source with temperatures between 30 and 300K. The temperature of this blackbody was determined with a limited accuracy. The blackbody source was also extended with respect to the SWS slit, leading to diffraction losses, so a difference could be expected in the Relative spectral response as measured in the lab and on a point-source.

In March 1997 a new series of CAL25s was derived (version numbers 20) by applying polynomial broadband corrections to the existing CAL25 files (versions 10), based on the differences between SWS spectra of standard stars and reference spectral energy distributions, mostly synthetic spectra from star models and composites (i.e. pieces of synthetic spectra and real data spliced to accurate photometry available). These calibration files are available in IA as cal25_*_020.

4.1 band 1a

Correction : Polynomial (degree 3) based on the following observations and SEDs :

Source	TDT	SED
HR5340	45200101	HR5340_M_MRCS1
HR6705	37704637	HR6705_M_IRFM_MRCS
HR7001	17800501	HR7001_M_MRCS1
HR4534	04001710	HR4534_M_KRZ_MORRS
HR7310	20601232	HR7310_M_MRCS1
HR8775	20601346	HR8775_M_COHEN

4.2 band 1b

Correction : Polynomial (order 3) based on the following observations and SEDs :

Source	TDT	SED
HR5340	45200101	HR5340_M_MRCS1
HR6705	37704637	HR6705_M_IRFM_MRCS
HR7001	17800501	HR7001_M_MRCS1
HR4534	04001710	HR4534_M_KRZ_MORRS
HR7310	20601232	HR7310_M_MRCS1
HR8775	20601346	HR8775_M_COHEN

4.3 band 1d

Polynomial correction (order 3) based on the following observations and SEDs :

Source	TDT	SED
HR5340	45200101	HR5340_M_MRCS1
HR6705	37704637	HR6705_M_IRFM_MRCS
HR7001	17800501	HR7001_M_MRCS1
HR7310	20601232	HR7310_M_MRCS1
HR8775	20601346	HR8775_M_COHEN

4.4 band 1e

Polynomial correction (degree 4) based on the following observations and SEDs :

Source	TDT	SED
HR5340	45200101	HR5340_M_MRCS1
HR6705	37704637	HR6705_M_IRFM_MRCS
HR7001	17800501	HR7001_M_MRCS1
HR7310	20601232	HR7310_M_MRCS1
HR8775	20601346	HR8775_M_COHEN

4.5 band 2a

Polynomial correction (degree 4) based on the following observations and SEDs :

Source	TDT	SED
HR5340	45200101	HR5340_M_MRCS1
HR8775	20601346	HR8775_M_COHEN

4.6 band 2b

Polynomial correction (order 3) based on the following observations and SEDs :

Source	TDT	SED
HR5340	45200101	HR5340_M_MRCS1
HR6705	37704637	HR6705_M_IRFM_MRCS
HR7001	17800501	HR7001_M_MRCS1
HR7310	20601232	HR7310_M_MRCS1
HR8775	20601346	HR8775_M_COHEN

4.7 band 2c

Polynomial correction (degree 2) based on the following observations and SEDs :

Source	TDT	SED
HR5340	45200101	HR5340_M_MRCS1
HR8775	20601346	HR8775_M_COHEN

4.8 band 3a

Polynomial correction based on the following observations and SEDs :

Source	TDT	SED
HR5340	45200101	HR5340_M_MRCS1
HR6705	04002405	HR6705_M_IRFM_MRCS
HR6705	37704637	HR6705_M_IRFM_MRCS
HR8775	20601346	HR8775_M_COHEN

4.9 band 3c

Polynomial correction based on the following observations and SEDs :

Source	TDT	SED
HR5340	45200101	HR5340_M_MRCS1
HR8775	20601346	HR8775_M_COHEN

4.10 band 3d

Polynomial correction (order 2) based on the following observations and SEDs :

Source	TDT	SED
HR5340	45200101	HR5340_M_MRCS1
HR8775	20601346	HR8775_M_COHEN

4.11 band 3e

Correction : Polynomial (order 2) based on the following observation and SED :

Source	TDT	SED
NML-CYG	05200726	NML-CYG_M_COHEN

4.12 band 4

Due to a lack of suitable observations (i.e. a decent S/N) of calibration targets with a well known energy distribution in the region 30-45 μm, no correction was applied on the RSRF for band 4.

5 ILT blackbody scan reprocessing

The first set of RSRFs was derived from the pre-launch blackbody scans without applying crosstalk correction. Since the entire DSPD part of the pipeline was changed in the course of 1997, also other small differences could be expected, so it was decided to re-process the data of the ILT blackbody scans using state-of-the art processing software before applying further corrections based on what was

ILT file	T(BB)	Ap	scan (lvdt)	band	lambda range
ILT5_MPE_TPF72_1	58.1K	2		3d	
				4d	
ILT5_MPE_TPF72_2	58.1K	3		3e	
				4	
ILT5_MPE_TPF72_3	81.2K	2		2a*	
				3c	
				4c	
ILT5_MPE_TPF72_4	101.6K	1		3a	
				4a	
ILT4_MPE_TPF72_1	150K	3		2c	
ILT4_MPE_TPF72_2	173K	2		2b	
ILT4_MPE_TPF72_3	261K	2		1d	
				1e	
				2a	
ILT4_MPE_TPF72_4	328K	1		1a	
				1b	

Table 1: Overview of ILT blackbody scans.

seen in-orbit. Below we describe the available data and the way this data can be used to produce RSRFs.

5.1 Available data

Table 1 shows an overview of the available datasets of the full blackbody scans obtained during the ground tests at Instrument Level. Although valid data for band 2a appears in ILT5_MPE_TPF72_3 it should not be used for that band since the blackbody temperature is too low to get a high signal in that wavelength region. ILT4_MPE_TPF72_3 should be used instead.

The ILT blackbody scan data are available in raw format as ltdf files in the MPE ILT MOD archive. They are also available in FITS format, processed to SPD level on the SWS consortium web pages in Leuven (http://sws.ster.kuleuven.ac.be) The ILT data was acquired on a little endian machine, so the data has to be bit-swapped when reading in the ltdf file on a big endian machine.

5.2 Wavelength calibration

The wavelength calibration between two warm-ups of the instrument changes drastically (order of 15 steps in LVDT). Therefore, it is important to use the proper wavelength calibration files as derived by Edwin Valentyn from the full grating calibrator scans made during the ILT tests. An overview is given in Table 2.

5.3 The dark current subtraction

Proper dark current measurements are available in the ILT data, but they are not properly flagged. A blackbody scan TPF has a dark block of the same gain and same reset interval before the scan,

ILT period	calfile	to be inserted in IA as	Former location on ISOW37
ILT4	cal16a	cal16a_ilt4(TBD)	IAS_ROOT:[arc.fm_ilt4]cal16a.fits
ILT4	cal16b	cal16b_ilt4(TBD)	IAS_ROOT:[arc.fm_ilt4]cal16b.fits
ILT4	cal16c	cal16c_ilt4(TBD)	IAS_ROOT:[arc.fm_ilt4]cal16c.fits
ILT4	cal16d	cal16d_ilt4(TBD)	IAS_ROOT:[arc.fm_ilt4]cal16d.fits
ILT4	cal16e	cal16e_ilt4(TBD)	IAS_ROOT:[arc.fm_ilt4]cal16e.fits
ILT5	cal16a	cal16a_ilt5(TBD)	IAS_ROOT:[arc.fm_ilt5]cal16a.fits
ILT5	cal16b	cal16b_ilt5(TBD)	IAS_ROOT:[arc.fm_ilt5]cal16b.fits
ILT5	cal16c	cal16c_ilt5(TBD)	IAS_ROOT:[arc.fm_ilt5]cal16c.fits
ILT5	cal16d	cal16d_ilt5(TBD)	IAS_ROOT:[arc.fm_ilt5]cal16d.fits
ILT5	cal16e	cal16e_ilt5(TBD)	[bart.work.cal25]cal16e.fits

Table 2: Wavelength calibration for the ILT blackbody scans

and a similar but shorter block after the scan. The first half of the latter suffers from memory effects after the high signal of the scan. To eliminate these effects, only the middle of the first block, and the last part of the second block should be flagged as DARK.

5.4 Spurious data

Spurious data in the ILT data is sometimes not flagged properly. Making a wavelength/grating position plot helps to select out these data-points and flag them as NODATA.

5.5 Dividing by a Planck function

The final step is then to divide the data by the expected energy distribution, i.e. a Planck function for the temperature of the blackbody at the time of the measurement.

6 Spline-smooth correction

Fitting the differences between observed and synthetic spectra using polynomes is not optimal. Allowing the polynome to fit the residues accurately in one part of the band immediately implies allowing it to fit the residues in other parts of the band with the same accuracy. Cubic Spline smoothing is therefore a better way of obtaining a continuous curve which is a good correction because it contains all the differences between observed and synthetic spectra that are understood to be instrumental. Cubic splines are continuous in all the knots, thus minimizing the risk of introducing false spectral features. cubic spline smoothing allows to specify for every knot the energy in the second order derivative. This means the stiffness of the smoothing curve can be changed in certain wavelength ranges. In regions where differences between observed and synthetic spectra are not understood, or not well reproduced across calibration stars of different spectral type or brightness, the smoothing curve will be kept stiff, and only a broadband correction will be applied. In regions where a small feature is known to be a RSRF residual, the parameters for the knots in that region will be relaxed and the smoothing curve will be allowed to follow the small feature.

In the fall of 1997, this approach was taken to derive a new set of RSRF calibration files, version 30. More data of known calibration stars had been gathered by then, so the improved residue fitting was combined with a better sampling of different spectral types, minimizing the risk that RSRF problems rather than imperfections in the synthetic spectra were corrected for.

For every AOT-band a set of suitable observations of know standard stars and corresponding synthetic spectra were selected. For each of these observations, the spectrum in every detector was divided by the synthetic spectrum at a resolution of $R/\delta R$ of 250. The residues of several stars were then combined into one average residue. Possible bias by spectral features not properly modeled in the synthetic spectra of stars of a specific spectral type were avoided by applying a sigma-clipping on the residues in every resolution bin before averaging.

The resulting averaged residue was then used as input for a parameterized cubic spline smoothing algorithm. The local parameters for each knot were chosen in a way to adapt the stiffness of the fit to the reliability of the residues in that region.

Below, an overview is given of the observations and synthetic spectra used to derive versions 30 of the cal25 files by spline smoothing correction of the ILT RSRF functions, re-derived as described in the previous section. Versions 40 are identical to versions 30, only the standard deviation field is made compatible with the error propagation in the pipeline. The overview below thus describes the observations used for the RSRF calibration in the present version of the standard product pipeline at the ISO Data Centre, IA and OSIA.

6.1 Band 1A

The following observations and model/composite SEDs were used:

Source	TDT	SED
HR1457	63602102	HR1457_M_COHEN
HR2491	68901202	HR2491_M_COHEN
HR5340	45200101	HR5340_M_MRCS1
HR7001	17800501	HR7001_M_HR_COHEN
HR7310	20601232	HR7310_M_MRCS1
ALF-CEN	60702006	ALFCEN_M_COHEN

Only broadband shapes in the residues were applied as a correction to the RSRF.

6.2 Band 1B

The following observations and model/composite SEDs were used:

Source	TDT	SED
HR1457	63602102	HR1457_M_COHEN
HR2491	68901202	HR2491_M_COHEN
HR5340	45200101	HR5340_M_MRCS1
HR6705	37704637	HR6705_M_IRFM_MRCS1
HR7001	17800501	HR7001_M_HR_COHEN
HR7310	20601232	HR7310_M_MRCS1
ALF-CEN	60702006	ALFCEN_M_COHEN

Only broadband shapes in the residues were applied as a correction to the RSRF.

6.3 Band 1D

The following observations and model/composite SEDs were used:

Source	TDT	SED
HR1457	63602102	HR1457_M_COHEN
HR2491	68901202	HR2491_M_COHEN
HR5340	45200101	HR5340_M_MRCS1
HR6705	37704637	HR6705_M_IRFM_MRCS
HR7001	17800501	HR7001_M_HR_COHEN
HR7310	20601232	HR7310_M_MRCS1
ALF-CEN	60702006	ALFCEN_M_COHEN

Only broadband shapes in the residues were applied as a correction to the RSRF.

6.4 Band 1E

The following observations and model/composite SEDs were used:

Source	TDT	SED
HR1457	63602102	HR1457_M_COHEN
HR2491	68901202	HR2491_M_COHEN
HR5340	45200101	HR5340_M_MRCS1
HR6705	37704637	HR6705_M_IRFM_MRCS
HR7001	17800501	HR7001_M_HR_COHEN
HR7310	20601232	HR7310_M_MRCS1
ALF-CEN	60702006	ALFCEN_M_COHEN

Only broadband shapes in the residues were applied as a correction to the RSRF.

6.5 Band 2A

The following observations and model/composite SEDs were used:

Source	TDT	SED
HR1457	63602102	HR1457_M_COHEN
HR2491	68901202	HR2491_M_COHEN
HR5340	45200101	HR5340_M_MRCS1
HR6705	37704637	HR6705_M_IRFM_MRCS
HR7001	17800501	HR7001_M_HR_COHEN
HR7310	20601232	HR7310_M_MRCS1
ALF-CEN	60702006	ALFCEN_M_COHEN

Only broadband shapes in the residues were applied as a correction to the RSRF.

6.6 Band 2B

The following observations and model/composite SEDs were used:

Source	TDT	SED
HR1457	63602102	HR1457_M_COHEN
HR2491	68901202	HR2491_M_COHEN
HR5340	45200101	HR5340_M_MRCS1
HR6705	37704637	HR6705_M_IRFM_MRCS
HR7001	17800501	HR7001_M_HR_COHEN
HR7310	20601232	HR7310_M_MRCS1
ALF-CEN	60702006	ALFCEN_M_COHEN

Only broadband shapes in the residues were applied as a correction to the RSRF.

6.7 Band 2C

The following observations and model/composite SEDs were used:

Source	TDT	SED
HR1457	63602102	HR1457_M_COHEN
HR2491	68901202	HR2491_M_COHEN
HR5340	45200101	HR5340_M_MRCS1
HR6705	37704637	HR6705_M_IRFM_MRCS
HR7001	17800501	HR7001_M_HR_COHEN
HR7310	20601232	HR7310_M_MRCS1
HR8775	55100705	HR8775_M_COHEN
ALF-CEN	60702006	ALFCEN_M_COHEN

Not only broadband shapes in the residues were applied as a correction to the RSRF. The local parameters were tuned to fit three narrow features which are believed to be instrumental since they are seen in all sources with the same strength and width. These three features were :

- 9-9.3 μm absorption
- 10.1 μm emission
- 11.0 μm emission

Be aware that these regions are still less reliable !

6.8 Band 3A

The following observations and model/composite SEDs were used:

Source	TDT	SED
HR1457	63602102	HR1457_M_COHEN
HR2491	68901202	HR2491_M_COHEN
HR5340	45200101	HR5340_M_MRCS1
HR6705	37704637	HR6705_M_IRFM_MRCS
ALF-CEN	60702006	ALFCEN_M_COHEN

In band 3A one small scale absorption feature at 12.3 μm was fit in the correction curve since it is believed to be an instrumental effect. The shape of the RSRF in this region is still less reliable than in the rest of the AOT band.

6.9 Band 3C

The following observations and model/composite SEDs were used:

Source	TDT	SED
HR1457	63602102	HR1457_M_COHEN
HR2491	68901202	HR2491_M_COHEN
HR5340	45200101	HR5340_M_MRCS1
HR6705	37704637	HR6705_M_IRFM_MRCS
ALF-CEN	60702006	ALFCEN_M_COHEN

Only broadband shapes in the residues are applied as a correction to the RSRF.

6.10 Band 3D

The following observations and model/composite SEDs were used:

Source	TDT	SED
HR1457	63602102	HR1457_M_COHEN
HR2491	68901202	HR2491_M_COHEN
HR5340	45200101	HR5340_M_MRCS1
HR6705	37704637	HR6705_M_IRFM_MRCS
ALF-CEN	60702006	ALFCEN_M_COHEN

Only broadband shapes in the residues are applied as a correction to the RSRF.

6.11 Band 3E

The following observations and model/composite SEDs were used:

Source	TDT	SED
HR1457	63602102	HR1457_M_COHEN
HR5340	45200101	HR5340_M_MRCS1
ALF-CEN	60702006	ALFCEN_M_COHEN
IRAS18162-2048	67801703	(interpol 3D and 4)

Only broadband shapes in the residues are applied as a correction to the RSRF.

In some AOT6 observations where the SW scan lasts longer than the LW scan (but not long enough to repeat up&down scan in the LW section) the LW scanning range is extended. Often band 3e data comes for free with the band 4 scan. This scan can extend over the official 3e ranges.

An observation on the compact HII region IRAS 18162-2048 was used where free band 3e data between 26 and 29.5 um was available. As model SED we used an interpolation between the band 4 and band 3D data. The agreement of the residues with residues of stellar sources makes us believe the interpolation is a valid assumption at the resolution we are rebinning to. (250)

6.12 Band 4

For band 4, no high signal observations of sources with known energy distribution in this wavelength region were available. Therefore, no correction for in-orbit differences are applied to the band 4 RSRF. Versions 30 and 40 contain the ILT RSRF reprocessed as described in the previous section.

7 Overview of the RSRFs and accuracies

In figures 3 to 14 we give an overview of the RSRF for one representative detector in every AOT-band. Below the RSRF a curve is plotted which shows an empirically determined uncertainty on the broadband shape of the RSRF. These uncertainties were determined by examining a large set of observations processed with the presented RSRFs and comparing them to the expected spectrum. As such, they do not contain a formal error, but rather an indication of the regions in the RSRFs which are known to be less reliable than other regions. The places where small-scale corrections to the ILT

RSRFs were applied can be recognized by a sudden raise in the uncertainty. Although these false features have been taken out, the risk of seeing a residue at these wavelengths is real.

The most important problems in the RSRF can be summarized as follows :

- Band 2C: 9-9.3 μm : possible residue of the correction for the instrumental absorption feature.
- Band 2C: 10.1 μm : possible residue of the correction for the instrumental emission feature.
- Band 2C: 11.0 μm : possible residue of the correction for the instrumental emission feature.
- Band 3A: 12.3 μm : possible residue of the correction for the instrumental emission feature.
- Band 3A, 3C, 3D, 3E : the fringes in bands 3 were also observed during the instrument level tests, so they are also present in the RSRF and will be divided out. However, the fringes in the RSRF are less resolved than in high resolution observations on point sources since the blackbody in the lab was extended to the SWS slit. Slight pointing errors will also result in a wavelength shift of the spectrum observed, so that the fringes can be slightly shifted wrt to the fringes in the RSRF, and this will result in fringe residues in the spectra.
- Band 3D: the red side of band 3D shows leakage from the wavelength region around 14 μm. Since the RSRF was corrected based on observations of stars that have a relatively high flux at 14 um, no proper correction of the RSRF in the leakage region was applied. In spectra of cold sources a false drop at the end of band 3D can be seen.
- Band 4 : no in-orbit correction has been applied due to lack of suitable observations/sources. It is now known that the lab measurements show a strong debiasing effect, and it can thus be expected that the shape of the current band 4 RSRF has a global inaccuracy of about 10

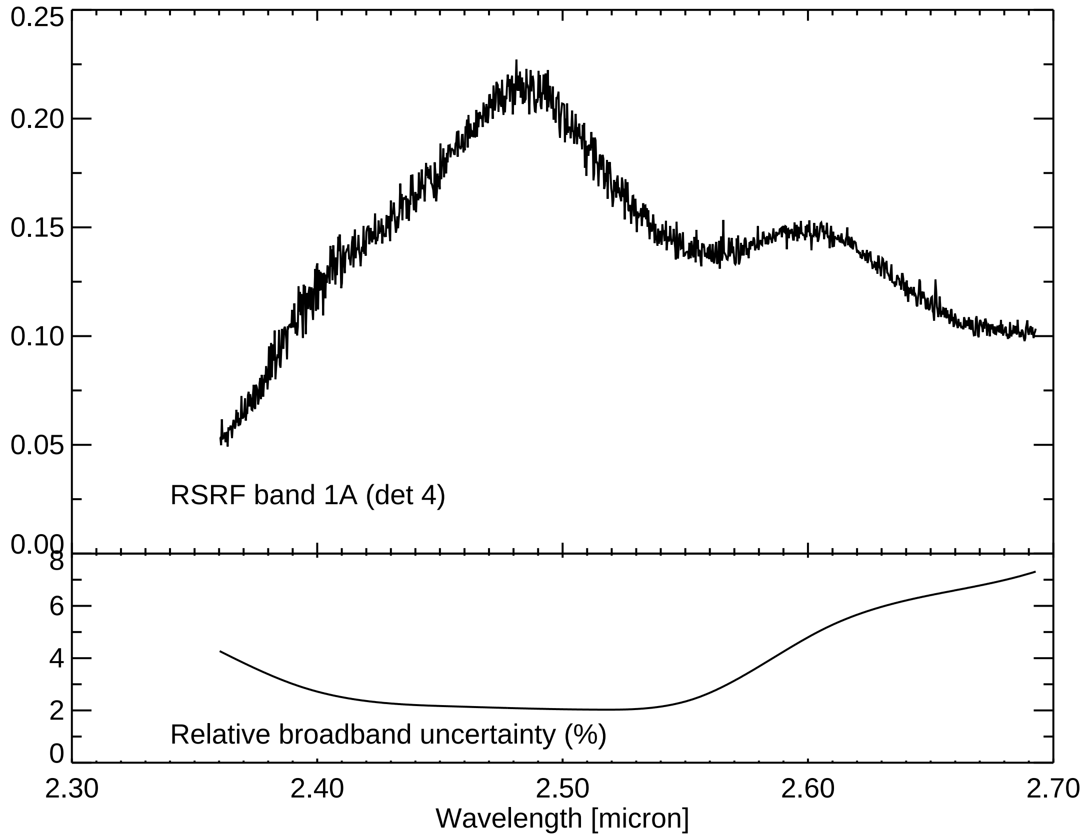

Figure 3: The RSRF for band 1A.

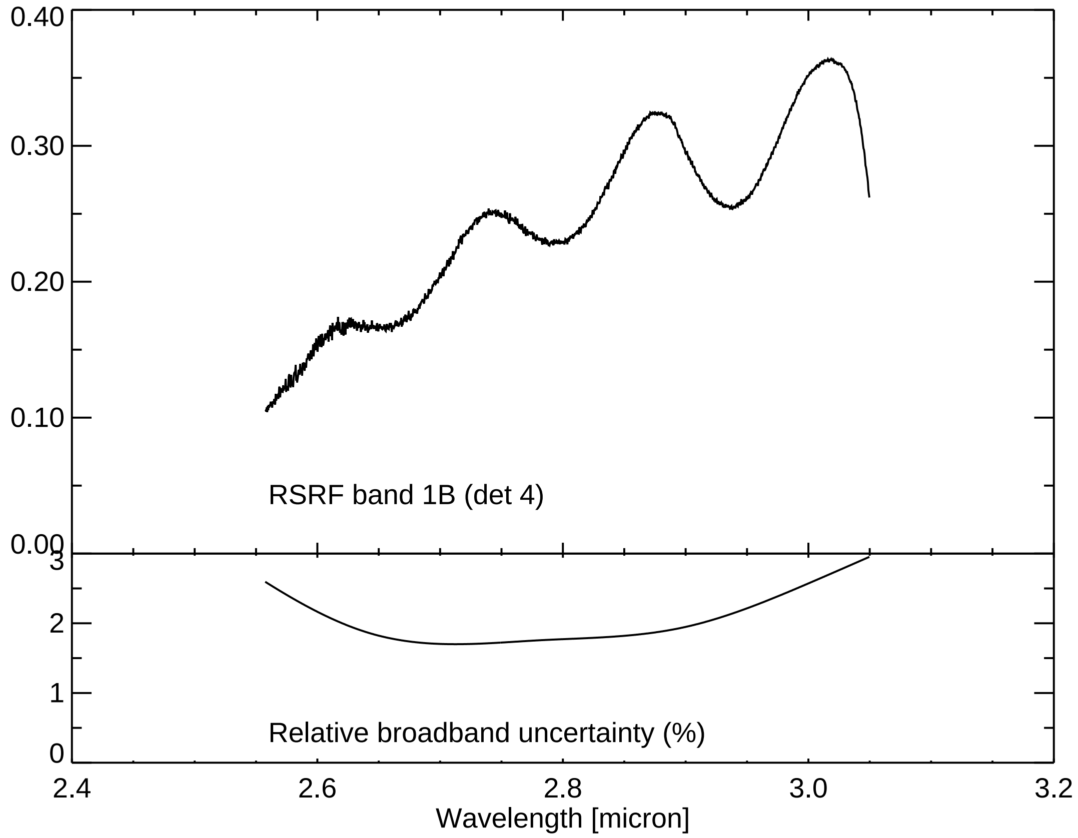

Figure 4: The RSRF for band 1B.

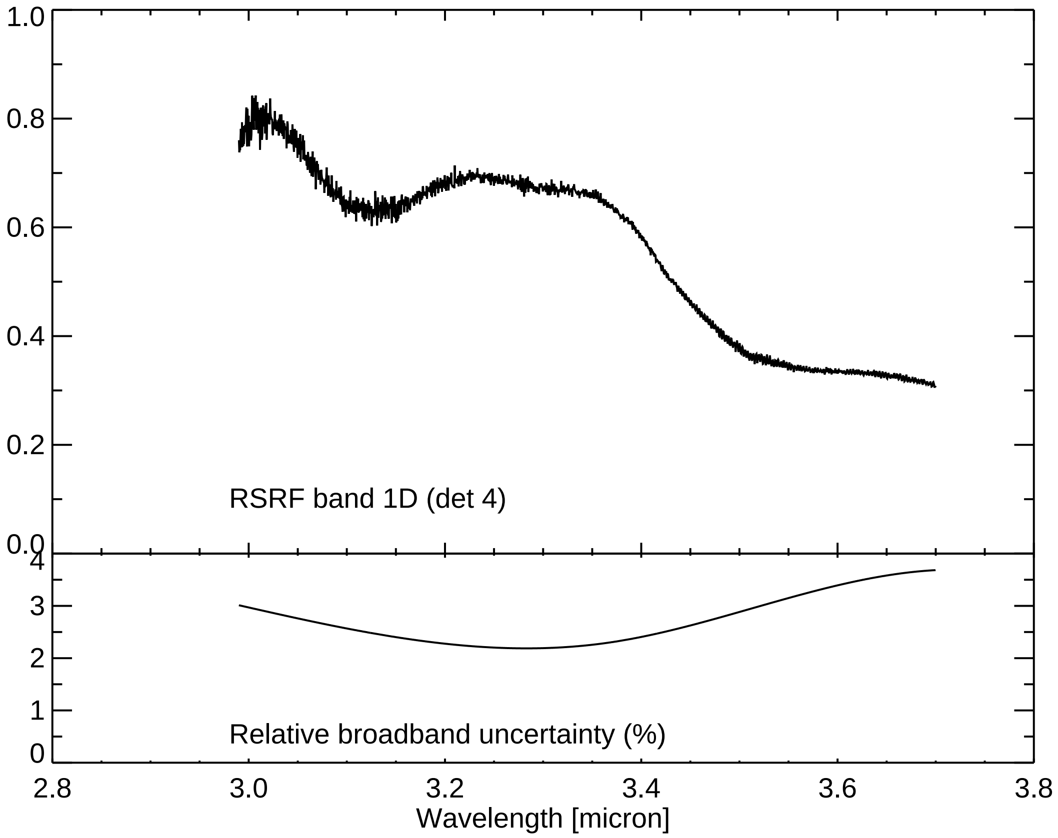

Figure 5: The RSRF for band 1D.

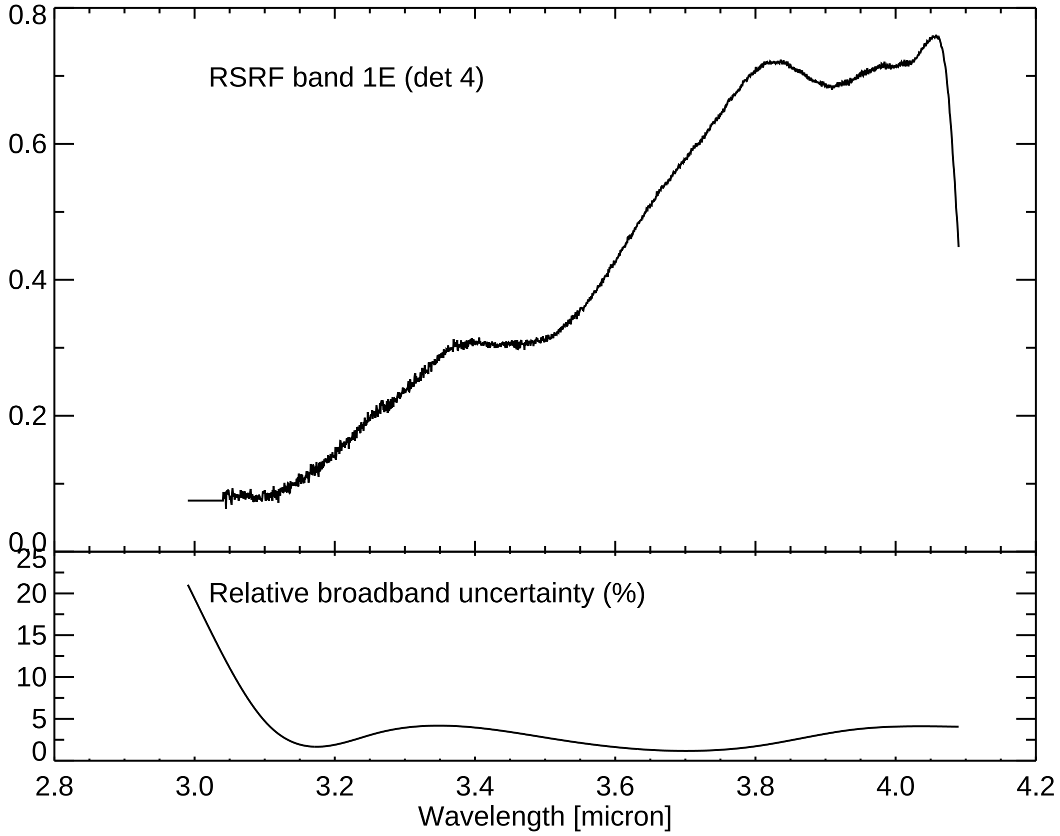

Figure 6: The RSRF for band 1E.

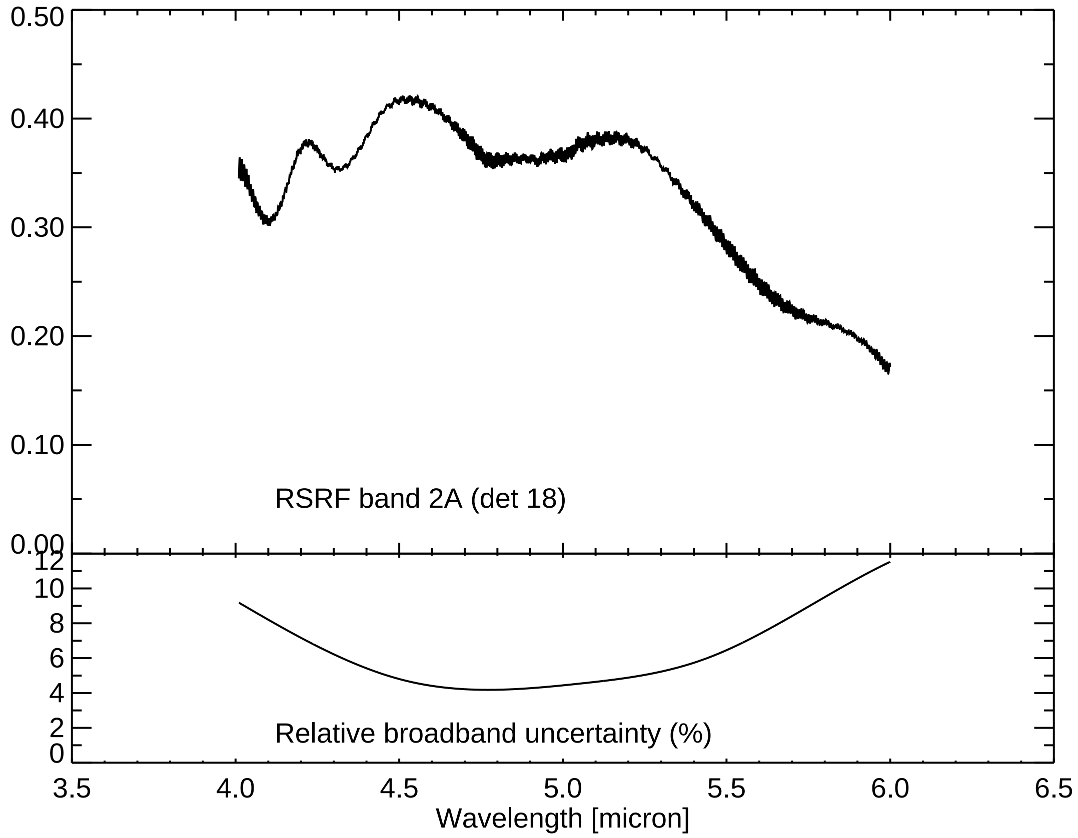

Figure 7: The RSRF for band 2A.

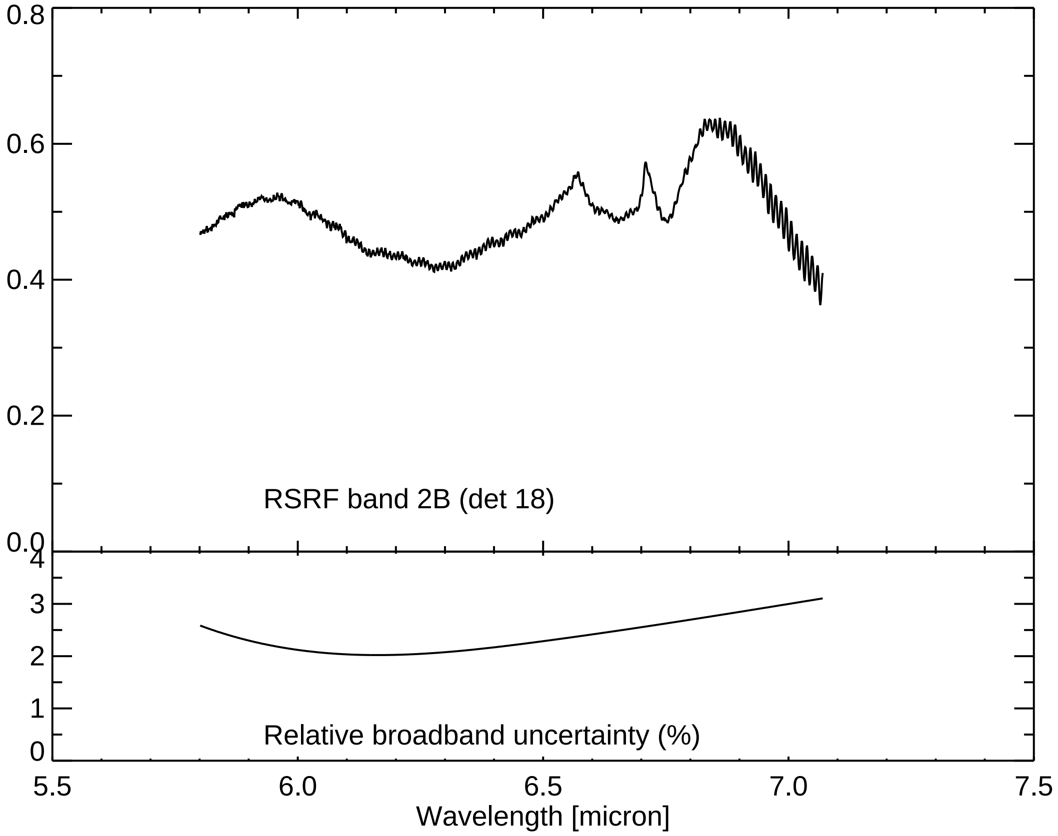

Figure 8: The RSRF for band 2B.

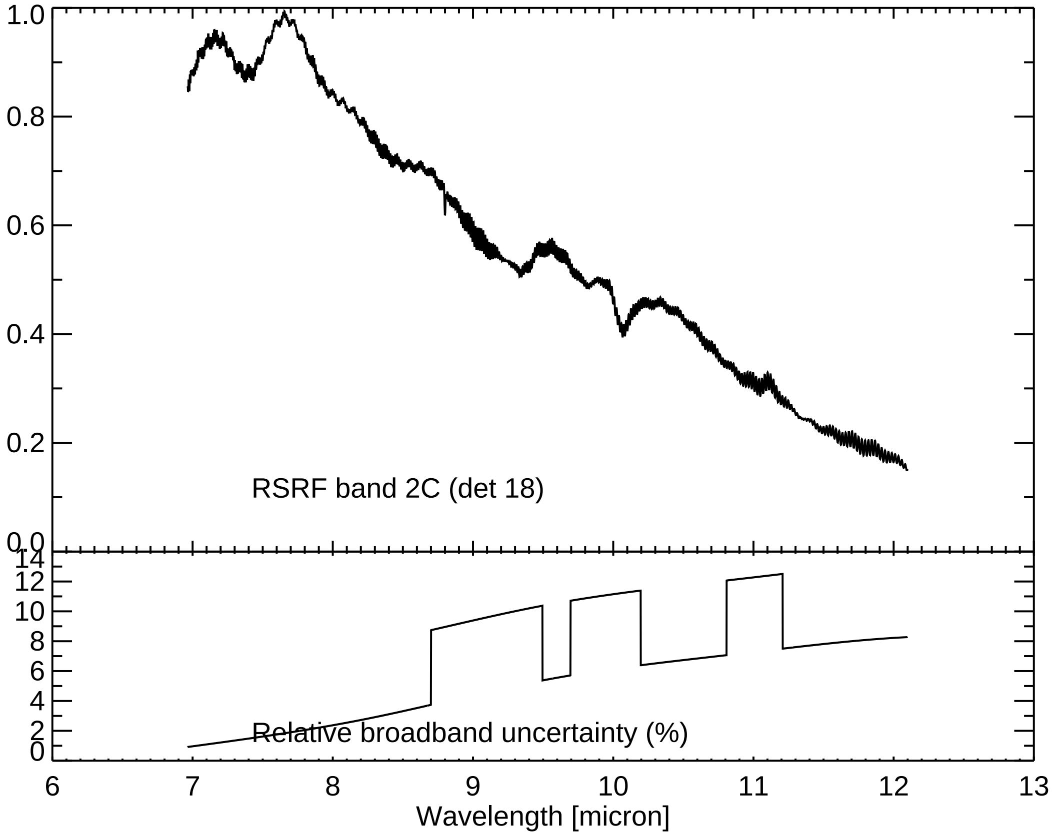

Figure 9: The RSRF for band 2C.

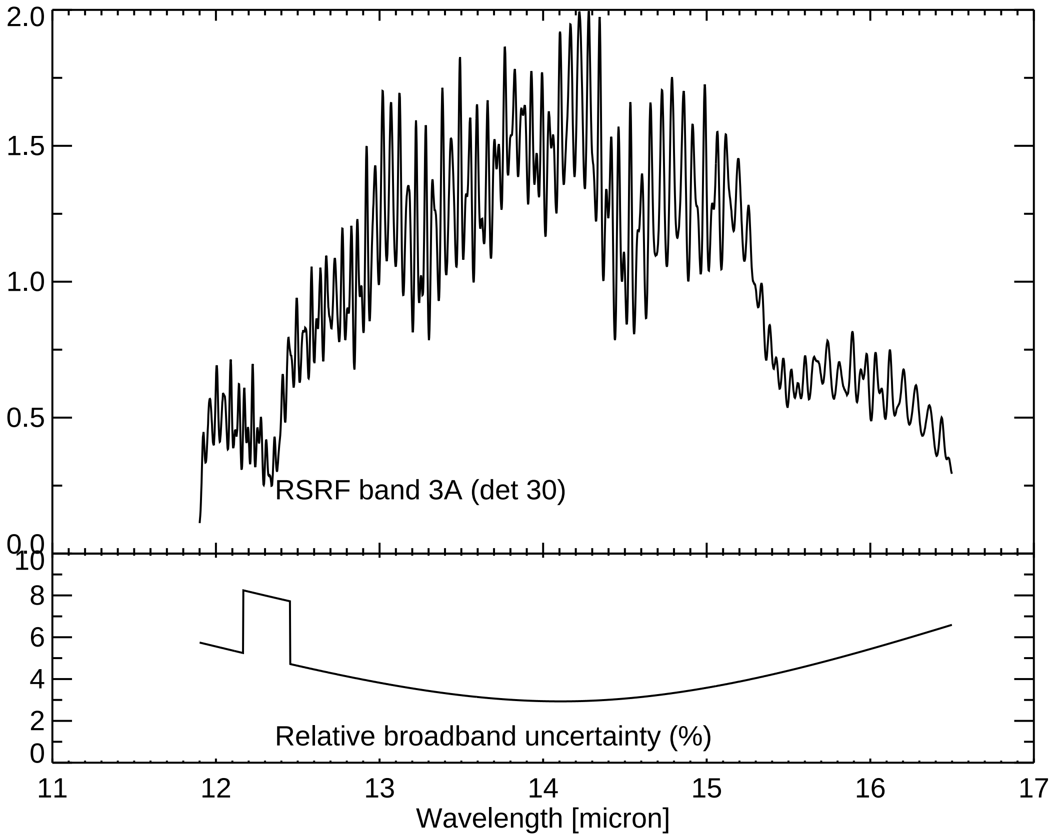

Figure 10: The RSRF for band 3A.

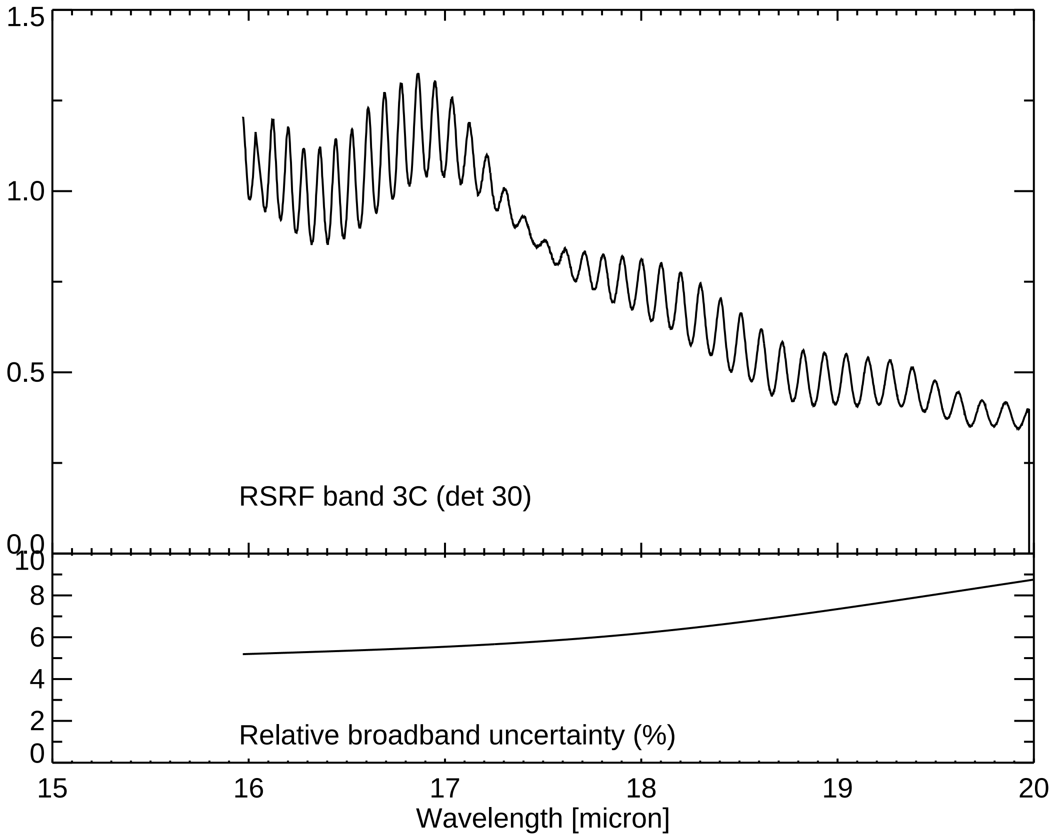

Figure 11: The RSRF for band 3C.

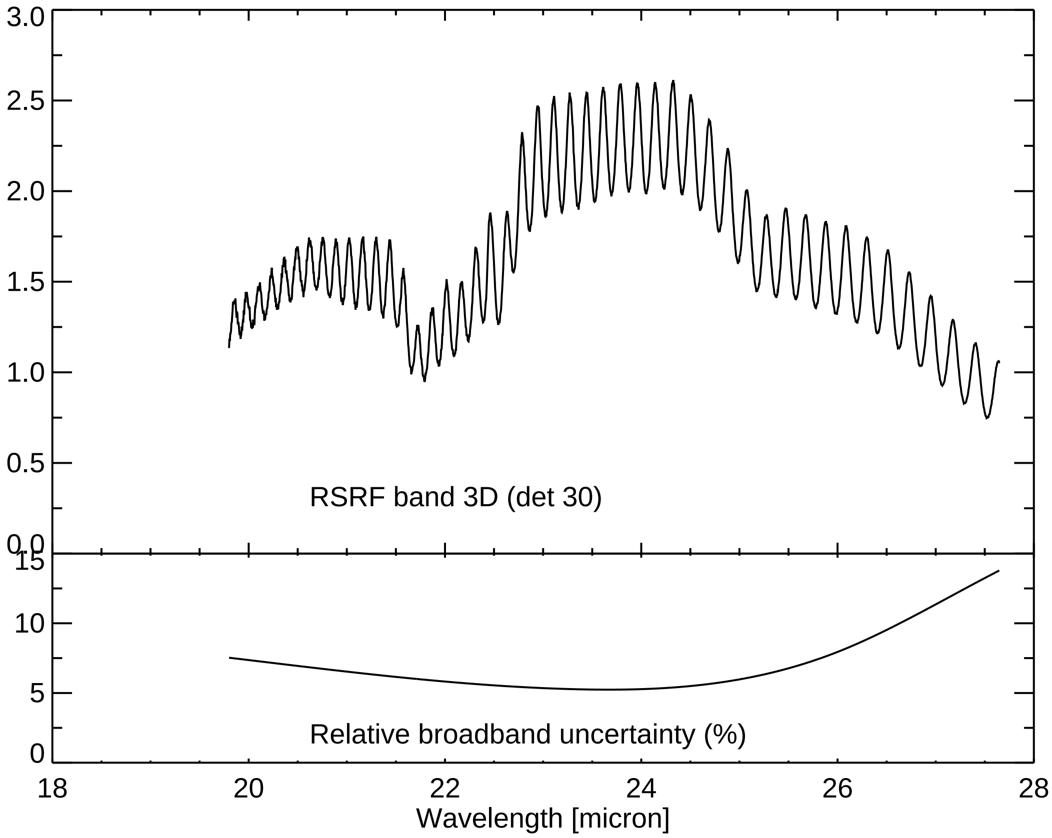

Figure 12: The RSRF for band 3D.

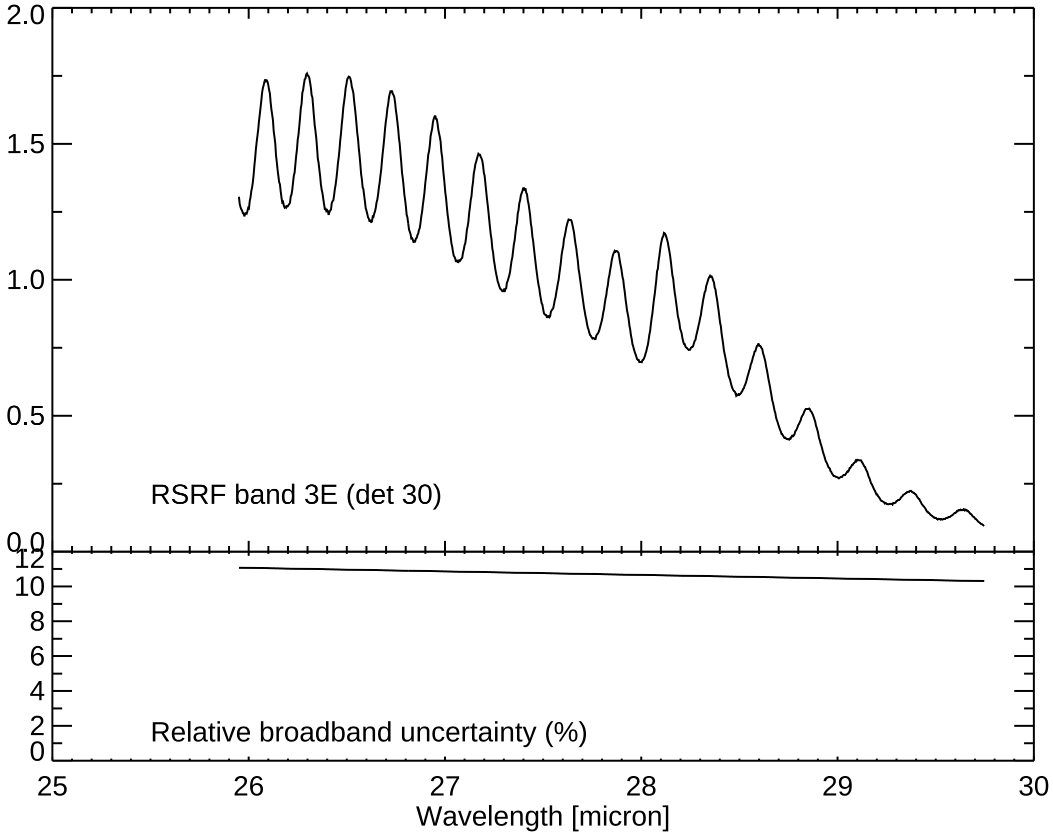

Figure 13: The RSRF for band 3E.

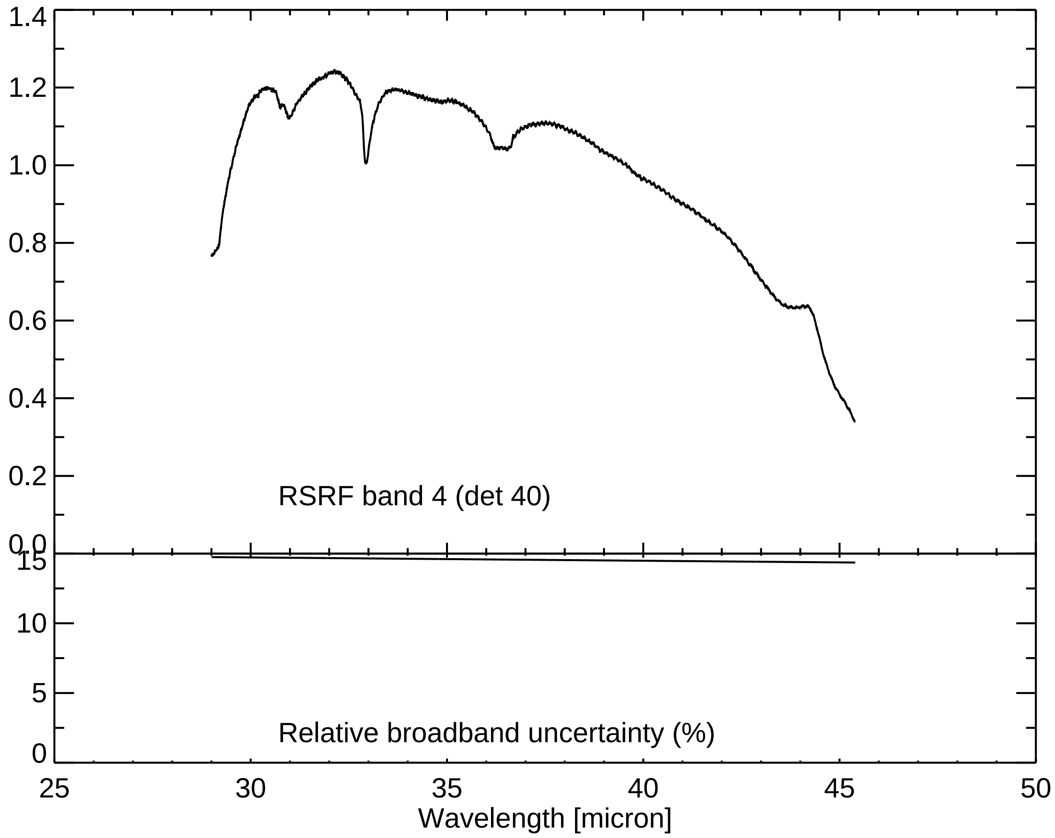

Figure 14: The RSRF for band 4.

8 RSRF features propagated to the spectra after wrong dark subtraction

The effect on the final spectrum of subtracting a wrong dark-current value depends on the RSRF in the wavelength region affected. The SWS RSRFS are not flat at all. They show steep slopes at the ends of the bands, and various bands show distinct features in their RSRF. The RSRF correction has to be applied on data for which a proper offset correction is done, i.e. the dark current subtraction has to be done properly. Dividing the data by the RSRF if the dark current subtraction was not done properly, will induce false shapes in regions where the RSRF shows features or where the RSRF has a steep slope. Poor matches between different AOT-bands can often be understood (and corrected for) from such a combination of dark current uncertainties and a steep RSRF in the overlap region. An example can be seen in figure 15. Shown is the original spectrum in band 3a (black, lower curve) and the spectrum in band 3c (blue). There is a clear discrepancy between the flux level and the slope of the spectrum in the overlap region. If we vary the dark current levels in the data with 10 % before applying the RSRF, we obtain the green spectrum for band 3a. The continuity of the spectrum at the band borders is much better now. 10 % is typically the difference between two dark current measurements in an observation, so it is not unreasonable to assume that the dark current measured for the 3a scan in this observation is off by 10 %.

The figures in the previous sections show where the RSRF is steep or shows features and thus where the risk for these artifacts exists. If the signal level of a scan is of similar strength than the dark currents for that band, it is wise to check if discontinuities at band overlaps or features whose position coincides with RSRF features are real or artifacts.

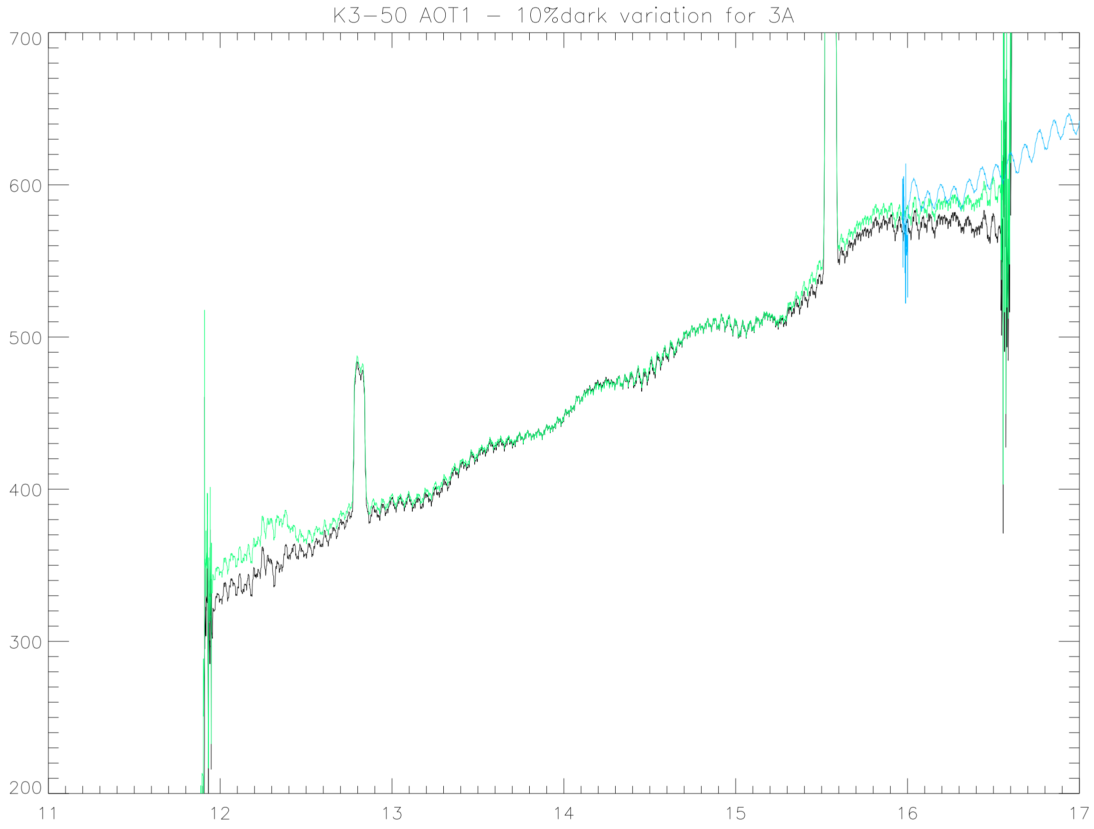

Figure 15: The shape of the band 3a spectrum of K3-50 before and after varying the dark current values with 10%.

9 Outlook

Improvements in the RSRF calibration of the SWS in the post-mission phase are expected in the following areas :

- Use of new and improved synthetic spectra to correct the ILT RSRF with spline-smoothing of residues between observed and synthetic spectra. Ongoing modeling work at the K.U.Leuven has resulted in a more reliable set of synthetic spectra for the most important SWS calibration stars in the short-wavelength section. These synthetic spectra are constructed from model atmospheres with the Uppsala non-LTE code. Currently, work is under way to improve the poor linelists for wavelengths $> 12\ \mu$m. This will eventually result in improved synthetic spectra for the long-wavelength bands.
- Extrapolation of the correction in the leakage region at the red side of band 3d, since verification on cold sources has shown that an extrapolation of the correction factors is better than no correction.
- Re-derivation of the RSRF for band 4 with proper debiasing correction of the ILT data. Debiasing has shown to be important at the signal levels of these data.
- Re-derivation of the RSRF for band 2 with proper memory effect correction of the ILT data.
- Re-derivation of the RSRF for all bands with improvements in the calibration at the slope level.

Appendix 1 - SEDs references

ALFCEN_M_COHEN

Calibrated model spectrum of Alpha[1] Centauri in calibrated template format. For details of the model and its absolute calibration see Cohen, M., Witteborn, F. C., Bregman, J. D., Wooden, D. H., Salama, A., & Metcalfe, L. 1996, "Spectral Irradiance Calibration in the Infrared. VI. 3–35 Micron Spectra of Three Southern Standard Stars", Astron.J. v.112, p.241 (1996)

HR1457_M_COHEN

Composite spectrum by Martin Cohen

Composite of observed spectra of Alpha Tau, assembled 03-19-92.

Spectral fragments and portions of these actually used in observed spectrum:

Fragment	Reference (μm)	Total range wavelengths (μm) Start and stop	
NIR	1	1.22- 5.50	1.22- 4.22
KAO-5-8	2	4.53- 9.38	4.53- 7.81
8-13	3	7.33-13.07	all
LRS	4	7.67-22.74	13.10-17.74
17-23	5	17.05-23.61	17.79-19.97
KAO-LONG	6	20.38-35.08	all

References: 1. Strecker, Erickson, and Witteborn 1979, Ap.J. Suppl, 41, 501. 2. NASA-Ames data principally of Dec. 20, 1991 KAO flight 3. Principally UKIRT data of Nov. 9, 1991 "service observations" for MC 4. IRAS Low Resolution Spectrometer, Groningen database 5. Entirely UKIRT data of Nov. 9, 1991 "service observations" for MC 6. Glaccum, unpublished Ph.D. dissertation observations (priv. comm. to MC),1990, Univ. of Chicago.

HR2491_M_COHEN

Composite spectrum by Martin Cohen

Composite of observed spectra of Sirius, assembled 07-91.

Calibrated model spectrum of Alpha CMa. For details of the model and its absolute calibration see Cohen, M., Walker, R.G., Barlow, M.J., and Deacon, J.R., 1992, "Spectral Irradiance Calibration in the Infrared, I., Astron. J. v 104, p 1650

HR4534_M_KRZ_MORRS

Kurucz model energy distribution by Pat Morris.

This model energy distribution is taken from Kurucz 1991 tables. The temperature (8750 K) and gravity (log g = 4.0) were found via best fit to near infrared (JKLN; Gezari et al., NASA RP-1294) and visual (Johnson & Mitchell Rev. Mex. Astron. Astroph. 1, 299) photometry. Solar abundances were adopted.

HR5340_M_MRCS1

Absolute calibrated spectrum of HR5340 version 1, 30.11.95

Atmosphere model: MARCS model with Teff = 4350K log g = 1.75 [M/H] = -.50

Synthetic spectrum: Uppsala SSG

Absolute calibration: at 2.202 mu: Fnu = 11030 Jy (Kn = -3.055)

HR6705_M_IRFM_MRCS

Absolute calibrated spectrum of HR6705. Version 1, 30.11.95

Atmosphere model: MARCS model with Teff = 4000K log g = 1.50 [M/H] = -0.25

Synthetic spectrum: Uppsala SSG

Absolute calibration: at 2.202 mu: Fnu = 2294 Jy (Kn = -1.350)

HR7001_M_MRCS1

Absolute calibrated spectrum of HR7001. Version 1, 30.11.95

Atmosphere model: Dreiling and Bell (1980): Teff =9650K log g = 3.90 [M/H] = 0.00

Synthetic spectrum: Uppsala SSG

Absolute calibration: at 555.6 nm: Fnu = 3563 Jy (V = +0.03)

HR7001_M_HR_COHEN

Composite spectrum by Martin Cohen

Calibrated model spectrum of Alpha Lyr. For details of the model and its absolute calibration see Cohen, M., Walker, R.G., Barlow, M.J., and Deacon, J.R., 1992, "Spectral Irradiance Calibration in the Infrared, I., Astron. J. v 104, p 1650

HR7310_M_MRCS1

MARCS model energy distribution, version 1, 30.11.95

Atmosphere model: MARCS model with Teff = 4800K log g = 2.75 [M/H] = -0.00

Synthetic spectrum: Uppsala SSG

Absolute calibration: at 2.202 um: Fnu = 328.5 Jy (Kn = +0.760)

HR8775_M_COHEN

Synthetic spectrum by Martin Cohen

Spectral fragments and portions of these actually used in observed spectrum

Fragment	Reference	Total range (μm)	Start and stop wavelengths (μm)
NIR	1	1.22- 5.70	1.22- 5.14
KAO-5-8	2	5.23- 8.06	all
8-13	3	7.50-13.07	8.13-13.07
LRS	4	7.67-22.74	13.10-21.00
LONG	5	1.25-35.00	19.45-35.00

References:

1. Strecker, Erickson, and Witteborn 1979, Ap.J. Suppl, 41, 501.

2. NASA-Ames data from August 5, 1986 KAO flight (Bet Peg cf. Alp Lyr) and from Nov. 27-28 and 28-29, 1990 KAO flights (Bet Peg cf. Alp Tau).

3. From UKIRT data of July 16, 1990 CGS3 data of M. Barlow (priv. comm. to MC), Mt Lemmon (Ames) data of Oct. 11 and 14, 1989 (Bet Peg cf. Alp Lyr), and UKIRT data of Oct. 5, 1990 (Bet Peg. cf. Alp Tau) from M. Barlow's CGS3 data (priv. comm. to MC) and previously defined Alp Tau 8-13 data.

4. IRAS Low Resolution Spectrometer, Groningen database

5. Engelke Fn. used for T=3600K (see Blackwell, Lynas-Gray, and Petford 1991, Astron. Astrophys., 245, 567); best

NML-CYG_M_COHEN

Synthetic spectrum by Martin Cohen

This is a "special" product assembled without benefit of [tracable] photometry.

The complete spectrum is tied to Glaccum's KAO long wavelength spectroscopy, absolutely calibrated on Mars (good to +/-2.5and secured with a large aperture. Glaccum spectra usually match well to other composites when joining to LRS or ground- based 20 um spectra. Note that there are some real features near 34 um (and perhaps also near 28 um) in the Glaccum data, also a potential silicate absorption at 10 um in the UKIRT spectrum.

This composite starts near 7.5 um and is continuous to 66 um. As such it is probably a useful tertiary (secondary?) calibrator for SWS, particularly in bands 3 and 4.

This cannot be regarded as a "high quality" absolute calibrator although its low-resolution shape is likely to be valid.

The plausible values of magnitudes near 10/20 um as follows (cf. the CIO): [8.7] = 5.0; N = -5.4; [11.7] = -5.8; [20] =-7.0.

Spectral fragments and portions of these actually used in observed spectrum ("used" may include combination with other data where overlaps occur)

Fragment	Ref	Tot range (μm)	beg - end (μm)	Avg resolving power
NIR	1	1.30- 4.00	not used	50
8-13	2	7.50-13.30	7.50-13.30	55
LRS	3	7.67-22.70	11.30-22.70	30
LONG	4	19.92-35.03	19.92-35.03	30
VLONG	5	35.19-65.80	35.19-65.80	30

References:

1. Strecker, unpublished KAO archives, NASA-Ames (unused here because there is no continuity with the other fragments).

2. UKIRT CGS3 data of October 7, 1992 [NML Cyg/beta Peg], both taken at airmass 1.17 by Sylvester & Skinner.

3. LRS raw data extracted from the old Groningen "LRSVAX" archive maintained at NASA-Ames and recalibrated correctly.

4,5. From Glaccum (1990): taken on the KAO flight of July 7, 1986 with the Goddard 24 channel He-3 bolometer spectrometer in two grating settings, and calibrated against Mars.

Appendix 2 - CAP6244

CAP6244 is used to derive a RSRF from an ILT black-body scan

```
;------------------------------------------------------------------------------
; check length of ltdf file with list in the MOD sleeve & read in the ltdf file
;------------------------------------------------------------------------------
e = readtdf("", s=13, n = 4800, /bswap)

; ---------------------------------------------------
; Use the right calfiles for wavelength calibration in ILT
; ---------------------------------------------------
cal\_select

; ----------------------------------------------------------
; write a timekey in the header to find the right time dependency
; for calibration files
; ----------------------------------------------------------
head = e.header
nhead=write\_fits\_key(head,'EOHAUTCS','97196153306', 'S', \$
'Approx. UTC of start of observation', stat)
e.header = nhead

; ----------------------------------------------------------
; Process to SPD
; ----------------------------------------------------------

s = dspd(e, aotn='s99')

; ------------------------------------------------------------------
; flag the right data as dark - check manually what points are good darks
; ------------------------------------------------------------------
s.data[20:150].status = \$
   make\_status(/dark, status=s.data[20:150].status)
s.data[4770:4795].status = \$
   make\_status(/dark, status=s.data[4770:4795].status)

; ---------------------------------------
; Subtract the dark currents from the data
; ---------------------------------------
sd = dark(s)

; -----------------------------------------
; Select the data to calculate the RSRF from
; -----------------------------------------
plotspd, sd, xax='wave', yax='grpos', band=4
```

```
sds = select(sd, sd.data.grpos(1) gt 3700 and sd.data.det(40).wave gt 11.)


; ----------------------------------------------------------------------
; Divide the data by a blackbody of the right temperature and get back the
; RSRF in a cal25* structure.
; ----------------------------------------------------------------------

c = c244\_respcal('4a', sds, temp=101.6)
```

Document Change Log

Version	Date	Edited by	Comment
1.0	24-oct-1999	BV	
1.1	26-oct-1999	BV	Introduced various paragraphs to make this document less opaque for the general observer, following KL suggestions.